First publ. in: Cellular and Molecular Life Sciences 61 (2004), pp. 2092-2099

Research Article

PrP^c and reggies/flotillins are contained in and released via lipid-rich vesicles in Jurkat T cells

A. Reuter *, U. Binkle, C. A. O. Stuermer and H. Plattner

Departments of Biology, Neurobiology and Cell Biology, University of Konstanz, 78457 Konstanz (Germany), Fax: +49 7531 88 3894, e-mail: alexander.reuter@uni-konstanz.de

Received 3 May 2004; received after revision 14 June 2004; accepted 23 June 2004

Abstract. A new model of caveolin association with lipid body cores has recently been proposed which may be relevant to a number of cellular processes, e. g. lipid body generation. Here we show that PrP^c and reggie-1 and reggie-2 also occur in the cores of Nile Red/Bodipy-stained (neutral lipid-containing) vesicular structures and, in immunoblots, in the lipid-enriched fraction after density gradient centrifugation. These lipid-rich vesicles increase in number following cell feeding with oleic acid, differ from early endosome antigen 1- and Lamp-2-positive endosomes/lysosomes, exhibit an opaque content and lack surrounding actin staining. Our results suggest that the content of these vesicles, together with reggie-1 and -2 and PrP^c, is expelled.

Key words. Cellular prion protein; reggie/flotillin; lipid-rich vesicle; release/exocytosis.

Reggie-1 and -2 (also known as flotillin-2 and -1) are detergent-resistant (DRM) plasma membrane-associated proteins of non-caveolar lipid raft microdomains in lymphocytes, neurons and many other cells [1–3]. Lipid rafts serve as platforms for the spatial concentration of glycosylphosphatidyl inositol (GPI)-anchored and (doubly) acylated intracellular proteins such as src tyrosine kinases, and effect signal transduction [4]. The cellular prion protein (PrP^c) as well as Thy-1 (both GPI-anchored proteins) are known to associate with rafts and colocalize with reggie rafts in caps during the induction of T cell activation [2, 5]. Moreover, they are jointly internalized into Limp-2-positive lysosomes and coexist in endosomes during their pathway through the cell [2; C. A. O. Stuermer, unpublished data]. The conversion of PrP^c into $PrP^{scrapie}$ (PrP^{sc}) has been suggested to occur in rafts or during its intracellular path through recycling compartments [6, 7]. Transfer to other cells seems to be mediated by cell-cell contact [8, 9] but release of PrP^c or PrP^{sc} particles has also been reported [10, 11] and may take place by unconventional modes of vesicle release [12–14]. In our analysis of reggies and PrP^c in Jurkat T cells we observed both of them in intracellular vesicles that are distinct from endosomes and lysosomes, but rich in neutral lipids (Nile Red and Bodipy 493/503 labeled). They are thus reminiscent of lipid-rich, caveolin-labeled vesicles – in caveolin-expressing hepatocytes and FRT cells – which bud from the endoplasmic reticulum (ER) and may serve to transport cholesterol and caveolin to the plasma membrane [15–17]. An association of PrP^c with caveolae has been reported in caveolin-expressing cells [18]. However, caveolin is absent from lymphocytes and neurons [1, 2, 4]. These lipid-rich vesicles also resemble the lipid droplets of CHO K2 cells, also implied in transport or storage of specific proteins [19]. Most analyses have found caveolin at the surface of lipid droplets [15–17] together with other lipid droplet-associated proteins. Recently, however, caveolin was also detected in the core of the lipid droplets [20, 21] and not only in the outer monolayer. Here we identified lipid-rich vesicles in Jurkat T cells that contain reggie-1, reggie-2 and PrP^c not only at

* Corresponding author.

their surface, but also in their core and whose contents appear to be released.

Materials and methods

Cells and reagents

Jurkat T cells were maintained in RPMI 1640 medium with 5% FCS at 5% CO_2. Lipid loading was performed overnight by adding 300 µM oleic acid as described elsewhere [17].

For all fluorescence microscopy experiments, Jurkat cells were attached to polylysine-coated coverslips. The cells were then fixed with 4% paraformaldehyde (PFA)/0.1% glutaraldehyde/0.5% digitonin in PBS for 1 h at 4 °C or with 4% PFA in PBS at room temperature (RT, 5 min) followed by an immersion in 0.05% Triton X-100 in PBS for 5 s. Primary antibodies (Abs) were anti-ESA (Transduction Laboratories, Lexington, Ky.) recognizing reggie-1 [2], anti-flotillin recognizing reggie-2 (Transduction Laboratories), anti-PrP^c pAb (kindly provided by A. Aguzzi, Zürich, Switzerland), anti-reggie-2 pAb [2], anti-PrP^c mAbs 6H4 (Prionics, Zürich, Switzerland) and 3F4 (Signet, Dedham, Mass.), anti-fyn pAb, and anti-EEA1 pAb (both Santa Cruz Biotechnology, Santa Cruz, Calif.), anti-lck pAb (Upstate Biotechnology, Lake Placid, N. Y.), anti-Lamp-2 mAb (Affinity Bioreagents, Golden, Colo.), anti-adipophilin mAb (Progen, Heidelberg, Germany), anti-synaptobrevin pAb recognizing synaptobrevin-1 from several species (R. Kissmehl and H. Plattner), and anti-Thy-1 mAb (Biotrend, Köln, Germany). Secondary Abs were goat anti-mouse Alexa-488, goat anti-rabbit Alexa-488 and donkey anti-rabbit Cy3 (all Jackson ImmunoResearch, West Grove, Pa.). AB-gold conjugates for electron microscope (EM) analyses were as described previously [2]. Nile Red, Sudan Black and Filipin were from Sigma Aldrich (St. Louis, Mo.).

Immunolabeling

After fixation and washes in PBS (× 3), cells were exposed to the primary and secondary Abs in 1% BSA/PBS (2.5 and 1 h, respectively, at RT) and either mounted directly or after lipid staining on microscope slides using Mowiol (Calbiochem, Bad Soden, Germany) with n-propylgallate as antifading agent. Immunolabeled/lipid-stained cells were analyzed in a confocal laser scanning microscope (LSM 510; Zeiss, Oberkochen, Germany). Images were acquired with the LSM 510 software and processed further with the use of Photoshop (Adobe Systems, San Jose, Calif.). Nile Red-stained cells were bleached (1 min) prior to analysis of the immunolabeling.

Lipid staining

Immunolabeled cells were exposed to 100 µM Nile Red, or, to verify lipid staining, to 1 µg/ml Bodipy 493/503 or 2.5 µg/ml Filipin in PBS (10 min, RT), to 0.2% Sudan Black (in 70% ethanol, 15 min) or to 0.3% Oil Red O (in 60% 2-propanol, 5 min).

Cell fractionation and blotting

Lipid-rich vesicles were isolated essentially as described before [22]. In brief, cells were disrupted by two 5-s pulses with a Branson sonifier (Branson, Danbury, Conn.) in sucrose-relaxation buffer. Nuclei and unbroken cells were sedimented at 800 g for 5 min at 4 °C. Supernatant (1.5 ml) was sequentially underlayered by 1.5 ml light Percoll-sucrose solution and 1 ml of heavy Percoll-sucrose solution and overlayered by 1 ml of 8% sucrose solution. Gradients were centrifuged in MLS-50 swinging-bucket rotors (Beckman, Wakefield, Mass.) at 55,000 g for 30 min at 4 °C. Gradient fractions of 1.0 ml were collected from the top.

Gradient fractions were separated under reducing conditions in SDS-PAGE. The separated proteins were blotted onto nitrocellulose membranes according to standard procedures and blocked twice with 1.5% BSA in TBST (10 mM Tris, 150 mM NaCl, 0.02% Tween, RT). The blots were then incubated with the primary Abs for either 1 h at RT or overnight at 4 °C and incubated with the respective peroxidase-conjugated secondary Abs for 45 min at RT. Detection was performed with the Supersignal chemiluminescence kit (Pierce, Rockford, Ill.).

Electron microscopy

For immunogold localization, cells were prepared essentially as described previously [2]. Briefly, cells were fixed in 8% formaldehyde + 0.1% glutaraldehyde in PBS (pH 7.4) for 1 h at 0 °C, washed in PBS + glycine and then in PBS. Pelleted fixed cells were stirred in 8% gelatine, centrifuged and impregnated overnight at 4 °C with 2.3 M sucrose and 20% polyvinyl pyrrolidone (PVP10). Frozen cell pellets were cryosectioned for incubation with the respective primary Abs, followed by different gold conjugates, i. e. 5-nm colloidal gold particles (Au_5) coated with protein A (pA) for detecting polyclonal Abs (reggie-2), or with $F(ab)_2$-derived from goat anti-mouse Abs to visualize monoclonal Abs (6H4 anti-PrP^c Ab, anti-reggie-1 Ab). Abs and gold conjugates were from sources previously specified [see above and ref. 2]. In addition, we applied goat Abs against actin (Santa Cruz Biotechnology), followed by rabbit anti-goat Ab-Au_5 conjugate (BioTrend, Cologne, Germany and Sigma, Taufkirchen, Germany) to cells after LR-gold embedding and UV polymerization at –35 °C. For ultrastructural analysis, aliquots were fixed in OsO_4 and embedded in Spurr's resin according to standard procedures. The size of lipid droplets in ultrathin sections was determined at defined magnifications, taking the average of smallest and largest extension. Since section thickness is negligible with respect to droplet size, true

size (2r) was calculated from apparent size (l_m) according to $l_m = r*\pi/2$.

Results

Our analysis of Jurkat T cells revealed the presence of vesicles which are labeled by Nile Red (fig. 1), Bodipy 495/503, Oil Red O and Sudan Black (data not shown) at the light microscopic (LM) level and which appear electron lucent at the EM level (fig. 2). Such features are typical of lipid-rich vesicles which are known to exist in many eukaryotic cells. Staining with filipin, a marker for cholesterol, did not show any significant staining of those vesicles (data not shown). Nile Red-labeled vesicles in cells without oleic acid treatment ranged in size from 0.3 to 2 µm with a mean of 0.94 ± 0.31 SD µm (n = 50). The size of lipid-rich vesicles in untreated cells, identified by their amorphous content at the EM level was 1.10 ± 0.36 SD µm (± 0.07 SE, n = 25), in good agreement with LM estimations.

We examined the localization of reggie-1, reggie-2 and PrP^c in conjunction with Nile Red by LSM analysis. Reggie-1 and reggie-2 were contained in a subpopulation of the Nile Red-labeled vesicle-like structures (fig. 1, 1st and 2nd row). Moreover, a subpopulation of the Nile Red-stained vesicles was labeled by PrP^c pAB (fig. 1, 3rd row). Clearly, Nile Red-labeled vesicles are more abundant than reggie/Nile Red or PrP^c/Nile Red doubly labeled vesicles.

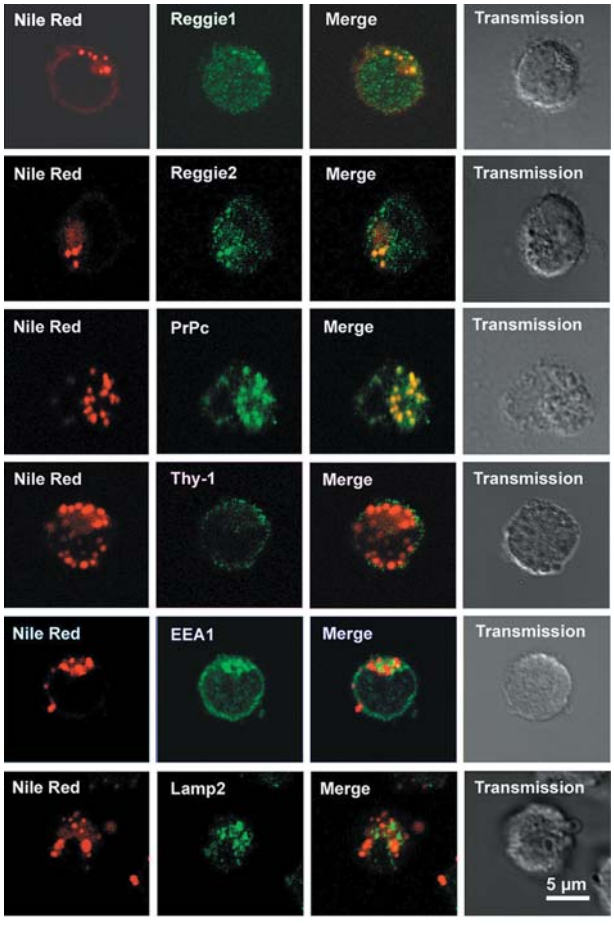

Figure 1. Colocalization of the lipid dye Nile Red with anti-reggie-1 and -2 and PrP^c labeling. In Jurkat T cells, the lipid dye Nile Red (first column) colocalizes with reggie-1 (first row), reggie-2 (second row) and PrP^c (third row). However, there is no colocalization with Thy-1 (fourth row), the endosomal marker EEA1 (fifth row) or the lysosomal marker protein Lamp-2 (last row). Scale bar, 5 µm.

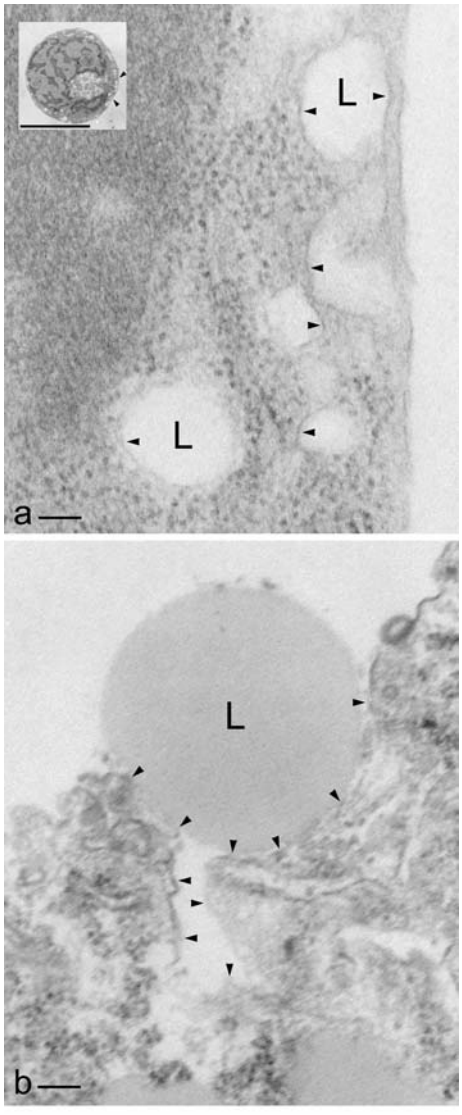

Figure 2. Identification of lipid-rich vesicles at the EM level. Standard plastic sections (epoxide) after OsO_4 fixation. Cell grown without (*a*) and with (*b*) oleic acid, resulting in larger, darker lipid vesicles. Scale bars, 0.1 µm. (*a*) Peripherally located lipid-rich vesicles (L) with membrane envelope (arrowheads). In the inset, arrowheads delineate the approximate position of the high-magnification image obtained from a consecutive section. Scale bar (inset), 10 µm. (*b*) Unstimulated lipid contents release. The outline of a membrane 'ghost' (arrowheads) is indicative of exocytosis.

Thy-1, another GPI-anchored protein of Jurkat T cells that is colocalized with reggie rafts, was not detected in Nile Red-positive vesicles (fig. 1, fourth row). Moreover, fyn and lck, two src family kinases, associated with reggie-1, reggie-2 and PrP^c in Jurkat T cell caps, also showed no colocalization with Nile Red-positive vesicles (data not shown). To exclude the possibility that the observed organelles are early endosomes or late endosomes/lysosomes which are known to contain reggie-1 and -2 as well as PrP^c, we stained Jurkat T cells with an Ab against EEA1 (fig. 1 fifth row) and Lamp-2 (fig. 1, sixth row) in conjunction with Nile Red. In this case, no colocalization was detected, so that the lipid vesicles in Jurkat T cells are unlikely to be endosomes or lysosomes.

To confirm that PrP^c and the reggies are associated with lipid vesicles, density gradient centrifugations modified to isolate lipid-loaded vesicles were performed. Reggies and PrP^c were detected by immunoblotting in the fraction 1 that contained most of the lipid-rich vesicles, as shown by detection of the lipid vesicle-associated protein adipophilin (fig. 3 A, B) and by microscopy (fig. 3 C). Interestingly, synaptobrevin-1, a protein required for docking and fusion of vesicles with membranes, also accumulated in the lipid vesicle-containing fraction 1 (fig. 3 B).

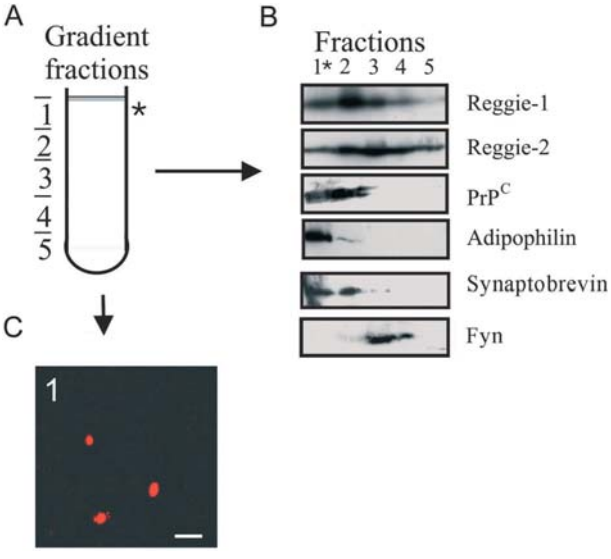

Figure 3. Density gradient fractionation of Jurkat T cells. After density gradient fractionation (*A*), lipid-rich vesicles accumulate in a fluffy layer at the top of the gradient (*). Reggies (48 kDa) are clearly present in fraction 1 (*) where most of the lipid-rich vesicles accumulate (*B*, row 1 and 2), as shown for fraction 1 by Nile Red staining at the LM level (*C*) and by adipophilin labeling (52 kDa, fourth row). PrP^c (33–35 kDa, third row) and synaptobrevin-1 (18 kDa, fifth row) accumulate in fractions 1 (lipid bodies) and 2 (non-lipidic, vesicular fragments, possibly microsomes). Fyn kinase (61 kDa), which is assocciated mainly with the cell membrane and endo-/lysosomes, accumulated in fractions 3 and 4 and showed no staining in the lipid-containing fraction 1 (last row). Scale bar, 3 μm.

Fyn kinase, a protein localized at the plasma membrane, in the cytosol and, to a lesser extent, in endo-/lysosomes, was included as a control and showed the expected accumulation in fractions 3 and 4 where most cellular vesicles reside (fig. 3 B).

Figure 4 shows typical examples of immunogold labeling of lipid-rich vesicles by Abs directed against reggie-1 and -2. Typical examples of lipid-rich vesicles which are labeled by anti-PrP^c mAbs are depicted in figure 5. Details shown in figures 4 and 5 are typical for lipid vesicles located at the cell periphery and they are labeled by the Abs.

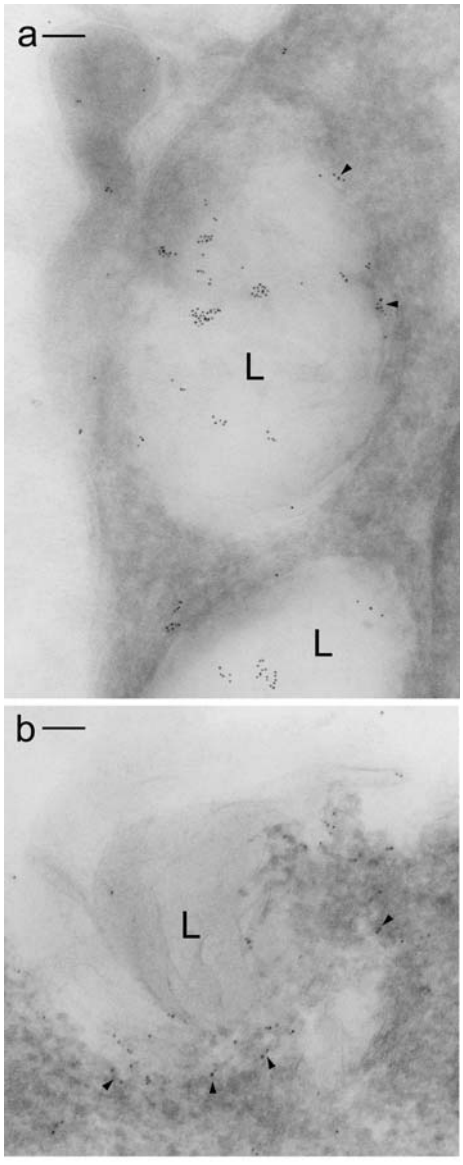

Figure 4. Reggie-1 and reggie-2 in lipid-rich vesicles (immunogold labeling). Cryosection with peripherally located lipid-rich vesicles (L) with reggie-1 (*a*) and reggie-2 (*b*) labeling. Labeling is not only along the vesicle boundaries (arrowheads), but also within lipid-rich vesicles. The situation depicted for reggie-2 suggests ongoing release of the labeled contents. Some label also occurs outside lipid-rich vesicles. Scale bars, 0.1 μm.

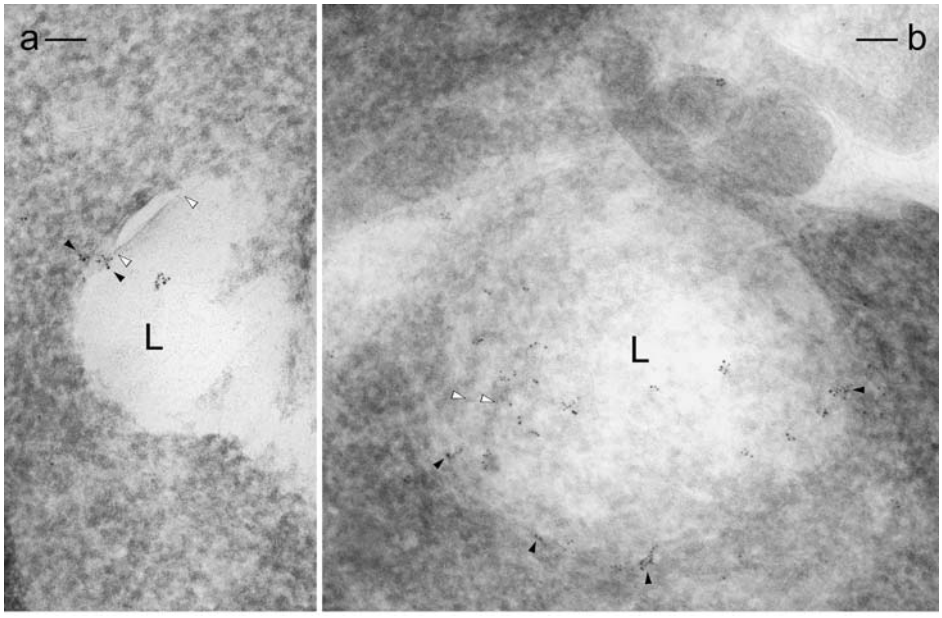

Figure 5. PrP^c in lipid-rich vesicles (immunogold labeling). Cryosection with PrP^c-labeled lipid-rich vesicles (L) located deeper within the cell (*a*) and at the cell boundary (*b*). Black arrowheads point to label associated with the vesicle membrane. (*a*) White arrowheads delineate a region where the vesicle membrane has been split. (*b*) Release of labeled contents in an omega-shaped profile typical for and suggestive of exocytosis. Scale bars, 0.1 µm.

Interestingly, labeling of lipid-rich vesicles by Abs against the reggies or PrP^c farther inside the cell was confined to the periphery of the vesicles (data not shown) whereas vesicles at the cell periphery showed more uniform labeling.

Such lipid vesicles not only closely approach the cell membrane, but are also seen as invaginations, suggesting ongoing exocytotic release (exemplified for reggie-1 and PrP^c labeling in figs 4 and 5 b, respectively) and accomplished release (as exemplified in fig. 4 b for reggie-2 labeling). This is consistent with a recent report showing the presence of proteins involved in vesicle trafficking and fusion in lipid-rich vesicles. While it appears unclear if all lipid droplets/vesicles are surrounded by a phospholipid mono- or bilayer, the lipid-rich vesicles shown here appear to possess a genuine membrane. This is suggested by our ultrathin cryosections where the limiting membrane is frequently detached from the lipid vesicle (contents) and sometimes appears split, as generally known from freeze-fractured membranes (fig. 5 a). Concomitantly, ultrathin sections of standard preparations, after osmication, clearly show a membrane structure (fig. 2 a). After oleic acid treatment, lipid vesicles increase in size and contents are released by exocytosis, with a 'membrane ghost' continuous with the cell membrane (fig. 2 b). Situations indicative of lipid-rich vesicle release were also encountered in LSM analysis (fig. 6, first row) where a Nile Red-positive vesicle is outside but associated with the main cell body suggesting the content of the vesicle was expelled.

Lipid loading of the Jurkat T cells resulted in a substantial increase in both number and size of the Nile Red- (and Bodipy 493/503)-positive vesicles (fig. 6, first row), which allowed their identification by phase contrast optics. Indeed, such vesicles were labeled by Abs against PrP^c and reggie-1 (fig. 6, second and third row). Neither reggie nor PrP^c increased upon lipid loading

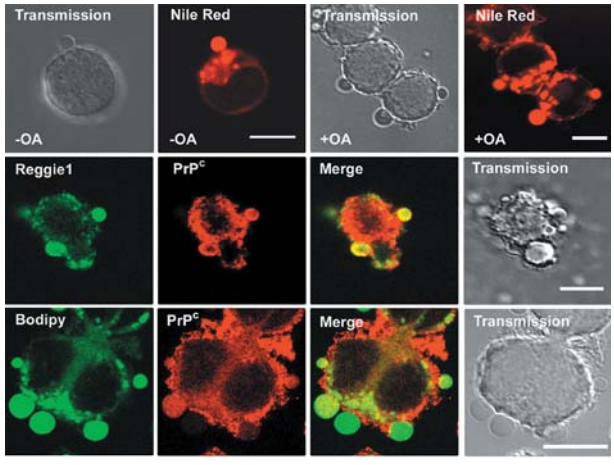

Figure 6. Lipid-rich vesicles outside the cell. Nile Red-stained Jurkat T cells, analyzed by LSM, exhibit a Nile Red-labeled vesicle associated with, but clearly outside the main cell body, suggesting vesicle release (row 1, panel 1 and 2). The occurrence of such vesicles increased (row 1, panel 3 and 4 and rows 2 and 3) after addition of oleic acid (+OA). Lipid-rich vesicles outside the cell are labeled by Abs against reggie-1 and PrP^c (row 2) and by neutral lipid dyes, such as Bodipy 493/503 staining (row 3). Scale bars, 5 µm

when fractions of lipid vesicles were analyzed (data not shown), but the occurrence of lipid vesicles outside the cell increased dramatically. Separating vesicles were relatively rare in untreated cells (fig. 6, first row) but abundant in oleic acid-treated cells by 6–8 h and even more after 24 h. Some of the Nile Red- and Bodipy-labeled lipid vesicles close to, but apparently outside the cell, were also labeled by PrP^c and reggie-1 Abs (fig. 6, second and third row). This suggests that Jurkat T cells transport and release the content of lipid-rich vesicles which increase in number upon addition of oleic acid, and deliver PrP^c and reggie into the medium. No such vesicles could be identified in the medium, thereby making uptake rather unlikely.

In accordance with vesicle release (rather than uptake) are our results with EM F-actin labeling. Only endocytotic, but not exocytotic vesicles are surrounded by F-actin. This also applies to large endocytotic vesicles, e.g. for macropinocytosis, which involves vesicles of similar size to the lipid-rich vesicles shown here. No corresponding actin labeling could be seen around lipid vesicles, even when labeling along the cell membrane and in filopodia was abundant (fig. 7), which is an additional argument for release by exocytosis.

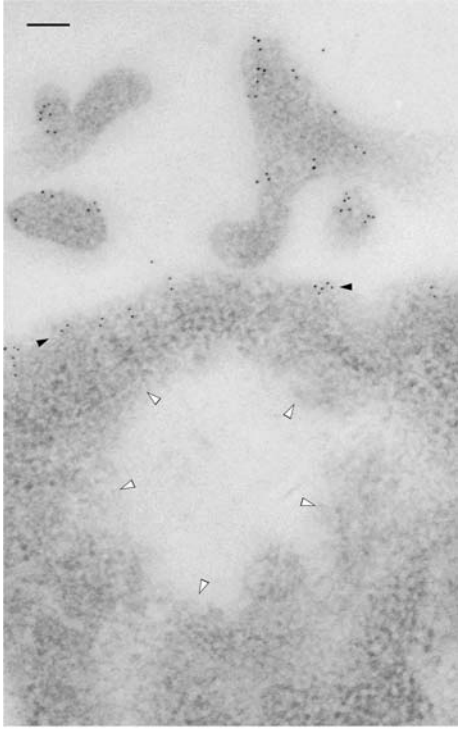

Figure 7. Absence of F-actin labeling from lipid-rich vesicles. LR-gold plastic section labeled with antibodies against F-actin, showing gold label in the numerous filopodia (top) and along the plasma membrane (between arrowheads), while no label occurs along the outlines of a lipid-rich vesicle (white arrowheads). While vesicle boundaries are lacking contrast because the section plane is not strictly median, this non-median section plane would facilitate the visualization of any surrounding actin halo (absent). Scale bar, 0.1 µm.

Discussion

Here, we show PrP^c, reggie-1 and reggie-2 to be localized within intracellular lipid-rich vesicles in Jurkat T cells. These vesicles were identified by four lipid dyes and found to increase in number and size upon loading of the cells with oleic acid. PrP^c and reggies occur together in the lipid-enriched adipophilin-labeled [19, 22, 23] fraction after gradient centrifugation. Nile Red- and Bodipy 493/503-positive vesicles inside the cell observed by immunofluorescence correspond in size and distribution to electron-lucent vesicles seen in our EM analysis, and both contain labeling with PrP^c-, reggie-1- and reggie-2-specific Abs. Vesicles close to the plasma membrane appear to release their content, most likely by exocytosis, implying that reggie-1 and -2, and most importantly, PrP^c, are expelled by the cell. This finding relates to reports showing that PrP^{sc} particles are transferred to distant cells acting as potentially infectious agents [8–10]. Lipid bodies also occur in CHO K2 cells and they contain flotillin/reggie [19] and also members of the Rab and SNARE family which allow vesicle transport and fusion [19]. We have identified synaptobrevin-1 in the lipid vesicle fraction of Jurkat cells which mediates membrane interaction for fusion [24], and, thus, also supports release of lipid vesicle contents by exocytosis.

Although it is unclear how the lipid-rich vesicles of Jurkat T cells in our study are generated, the proteins they contain, i.e. PrP^c and reggies, do possess lipid raft affinity and associate in plasma membrane rafts [1, 2]. Release of these proteins by lipid-rich vesicles appears rather unconventional, but osmium staining of membranes in ultrathin sections and apparent split membranes in cryosections around electron-lucent vesicles hint toward the fact that they are surrounded by a bona fide membrane, i.e. a lipid bilayer, as is required for release by exocytosis.

Reports on caveolin-1 and cholesterol transport in FRT cells and hepatocytes have shown the association of mutant caveolin-1 with Nile Red-labeled 'lipid droplets' [15, 16]. Lipid droplets, however, are thought to be surrounded by a phospholipid monolayer [25] enriched in certain proteins, such as a caveolin-1 mutant form [21]. Jurkat T cells do not express caveolin-1 [1, 2] but reggie-1 and reggie-2 in distinct patterns at the plasma membrane and intracellular compartments. Reggie and PrP^c are within the Nile Red-positive vesicles and close to the surrounding membrane. The more homogeneous labeling we find in peripherally located vesicles is considered realistic, because neither permeabilization nor dehydration solvents were used for cryo-EM. Internal staining of lipid droplets was also reported for caveolin in cryo-EM [20, 21]. Staining at the lipid vesicle margin in immunofluorescence may result from insufficient antibody penetration which would require thorough permeabilization to allow hydrophilic antibodies to reach the vesicle interior.

The detection of caveolin in the interior of lipid bodies [20, 21] and exclusively in the endoplasmic leaflet of ER membranes challenges the classic model of lipid droplet biogenesis. Traditional models assume that lipids initially accumulate between the endoplasmic and cytoplasmic leaflets of the ER membrane and that caveolin molecules reach the surface of the lipid droplet by lateral diffusion in the cytoplasmic leaflet of the ER membrane [20]. Finally, the lipid body buds off the ER. This hypothesis neither accounts for the presence of caveolin in lipid body envelopes because they are on the endoplasmic, wrong side of the ER membrane [20], nor for their presence in the lipid body cores. Instead, Robenek et al. [20] proposed a model in which caveolin is transferred by the lipids themselves into the droplet core during lipid droplet biogenesis, due to the high affinity of caveolin for cholesterol [20]. The situation for PrP^c is quite similar, as it has always been detected in the non-cytosolic surface of membranes, suggesting that transport of PrP^c and the reggies to the lipid-rich vesicle core may occur via a similar mechanism. The lipid-rich vesicles are most likely generated by fusion of smaller vesicles [18, 23], so that the surface-to-volume relation becomes increasingly smaller during the course of maturation by ongoing fusion. Therefore, this transfer process may be enhanced due to lack of surface space in the course of lipid body maturation. This would account for our observation that PrP^c and the reggies are preferentially localized in the periphery of the vesicles deep inside the cell, whereas they are distributed throughout vesicles which reside at the cell margin.

Evidence was provided earlier that, starting from rafts on the plasma membrane, reggies and PrP^c are jointly internalized in endosomes and Limp-2-positive lysosomes [2]. The lipid-rich vesicles observed here, however, were not labeled by the early endosomal marker EEA1 nor by Lamp-2, and thus are distinct from internalization compartments. The vesicles we observed are also rather unlikely to be incoming lipoproteins, because vesicles of this size have not been detected in the medium and because lipoprotein vesicles are generally considerably smaller (10–50 nm). In addition, low-density lipoprotein vesicle uptake takes place at coated pits which are easily identified at the EM level. Release is further supported by the absence of F-actin labeling around the electron-lucent, reggie- and PrP^c-positive vesicles at the EM level that appear as plasma membrane invaginations devoid of surrounding F-actin [26, 27]. Release of lipid vesicle contents containing reggie and PrP^c proteins by unstimulated exocytosis is therefore highly suggestive, especially as proteins of the Rab and SNARE family with functions in membrane transport and fusion have recently been detected in lipid droplet-containing fractions [18] where we found synaptobrevin-Ab binding in immunoblots. This opens the interesting possibility that propagation of prion infectivity may, in addition to cell contact-mediated pathways, also occur via release of prion-loaded lipid vesicles, and so participate in the neuroimmune transfer between follicular dendritic cells and sympathetic nerves that has recently been shown [28].

Acknowledgements. This work was supported by grants of the MWK TSE program Baden-Wuerttemberg and the DFG (TR SFB 11).

1 Lang D., Lommel S., Jung M., Ankerhold R., Petrausch B., Laessing U. et al. (1998) Identification of Reggie-1 and Reggie-2 as plasmamembrane-associated proteins which cocluster with activated GPI-anchored cell adhesion molecules in noncaveolar micropatches in neurons. J. Neurobiol. **37:** 502–523
2 Stuermer C. A. O., Lang D. M., Kirsch F., Wiechers M., Deininger S.-O. and Plattner H. (2001) Glycosylphosphatidyl inositol-anchored proteins and fyn kinase assemble in noncaveolar plasma membrane microdomains defined by reggie-1 and -2. Mol. Biol. Cell **12:** 3031–3045
3 Bickel P. E., Scherer P. E., Schnitzer J. E., Oh P., Lisanti M. P. and Lodish H. F. (1997) Flotillin and epidermal surface antigen define a new family of caveolae-associated integral membrane proteins. J. Biol. Chem. **272:** 13793–13802
4 Simons K. and Ehehalt R. (2002) Cholesterol, lipid rafts, and disease. J. Clin. Invest. **110:** 597–603
5 Simons K. and Toomre D. (2000) Lipid rafts and signal transduction. Nat. Mol. Cell Biol. **1:** 31–39
6 Vey M., Pilkuhn S., Wille H., Nixon R., DeArmond S. J., Smart E. J. et al. (1996) Subcellular colocalization of the cellular and scrapie prion proteins in caveolae-like membranous domains. Proc. Natl. Acad. Sci. USA **93:** 14945–14949
7 Naslavsky N., Stein R., Yanai A., Friedlander G. and Taraboulos A. (1997) Characterization of detergent-insoluble complexes containing the cellular prion protein and its scrapie isoform. J. Biol. Chem. **272:** 6324–6331
8 Liu T., Li R., Pan T., Liu D., Petersen R. B., Wong B.-S. et al. (2002) Intercellular transfer of the cellular prion protein. J. Biol. Chem. **277:** 47671–47678
9 Kanu, N., Imokawa, Y., Drechsel, D. N., Williamson, R. A., Birkett, C.R., Bostock, C.J. et al. (2002) Transfer of scrapie prion infectivity by cell contact in culture. Curr. Biol. **12:** 523–530
10 Gidon-Jeangirard C., Hugel B., Holl V., Toti F., Laplanche J.-L., Meyer D. et al. (1999) Annexin V delays apoptosis while exerting an external constraint preventing the release of CD4+ and PrPc+ membrane particles in a human T lymphocyte model. J. Immunol. **162:** 5712–5718
11 Parizek P., Roeckl C., Weber J., Flechsig E., Aguzzi A. and Raeber A. J. (2001) Similar turnover and shedding of the cellular prion protein in primary lymphoid and neuronal cells. J. Biol. Chem. **276:** 44627–44632
12 Vincent J.-P. and Magee T. (2003) Argosomes: membrane fragments on the run. Trends Cell Biol. **12:** 57–60
13 Kooyman D. L., Byrne G. W., McClellan S., Nielsen D., Tone M., Waldmann H. et al. (2003) In vivo transfer of GPI-linked complement restriction factors from erythrocytes to the endothelium. Science **269:** 89–92
14 Mehul B. and Hughes R. C. (1997) Plasma membrane targetting, vesicular budding and release of galectin 3 from the cytoplasm of mammalian cells during secretion. J. Cell Sci. **110:** 1169–1178
15 Fujimoto T., Kogo H., Ishiguro K., Tauchi K. and Nomura R. (2001) Caveolin-2 is targeted to lipid droplets, a new 'membrane domain' in the cell. J. Cell Biol. **152:** 1079–1085
16 Ostermeyer A. G., Paci J. M., Zeng Y., Lublin D. M., Munro S. and Brown D. A. (2001) Accumulation of caveolin in the endo-

plasmic reticulum redirects the protein to lipid storage droplets. J. Cell Biol. **152:** 1071–1078
17 Pol A., Martin S., Fernandez M. A., Ferguson C., Carozzi A., Luetterforst R. et al. (2004) Dynamic and regulated association of caveolin with lipid bodies; modulation of lipid body motility and function by a dominant negative mutant. Mol. Biol. Cell **15:** 99–110
18 Peters P. J., Mironov A. Jr, Peretz D., Donselaar E. van, Leclerc E., Erpel S. et al. (2003) Trafficking of prion proteins through a caveolae-mediated endosomal pathway. J. Cell Biol. **162:** 703–717
19 Liu P., Ying, Y., Zhao Y., Mundy D. L., Zhu M. and Anderson R.L. (2004) CHO K2 cell lipid droplets appear to be metabolic organelles involved in membrane traffic. J. Biol. Chem. **279:** 3787–3792.
20 Robenek M. J., Severs N. J., Schlattmann K., Plenz G., Zimmer K.-P., Troyer D. and Robenek H. (2004) Lipids partition caveolin-1 from ER membranes into lipid droplets: updating the model of lipid droplet biogenesis. FASEB J. Epub ahead of print.
21 Pol A., Luetterforst R., Lindsay M., Heino S., Ikonen E. and Parton R. G. (2001) A caveolin dominant negative mutant associates with lipid bodies and induces intracellular cholesterol imbalance. J. Cell Biol. **152:** 1057–1070.
22 Weller P. F., Monahan-Earley R. A., Dvorak H. F. and Dvorak A. M. (1991) Cytoplasmic lipid bodies of human eosinophils: subcellular isolation and analysis of arachidonate incorporation. Am. J. Pathol. **138:** 141–148.
23 Murphy D. J. (2001) The biogenesis and functions of lipid bodies in animals, plants and microorganisms. Prog. Lipid Res. **40:** 325–438.
24 Jahn R. and Südhof T. C. (1999) Membrane fusion and exocytosis. Annu. Rev. Biochem. **68:** 863–911.
25 Tauchi-Sato K., Ozeki S., Houjou T., Taguchi R. and Fujimoto T. (2002) The surface of lipid droplets is a phospholipid monolayer with a unique fatty acid composition. J. Biol. Chem. **277:** 44507–44512.
26 Becherer U., Moser T., Stuhmer W. and Oheim M. (2003) Calcium regulates exocytosis at the level of single vesicles. Nat. Neurosci. **6:** 846–853.
27 Sandvik K. and Deurs van B. (2002) Transport of protein toxins into cells: pathways used by ricin, cholera toxin and Shiga toxin. FEBS Lett. **529:** 49–53.
28 Prinz M., Heikenwalder M., Junt T., Schwarz P., Glatzel M., Heppner F.L. et al. (2003) Positioning of follicular dendritic cells within the spleen controls prion neuroinvasion. Nature **425:** 957–962.